# We are IntechOpen, the world's leading publisher of Open Access books Built by scientists, for scientists

## 6,900
Open access books available

## 186,000
International authors and editors

## 200M
Downloads

Our authors are among the

## 154
Countries delivered to

## TOP 1%
most cited scientists

## 12.2%
Contributors from top 500 universities

**WEB OF SCIENCE**™

Selection of our books indexed in the Book Citation Index
in Web of Science™ Core Collection (BKCI)

# Interested in publishing with us?
# Contact book.department@intechopen.com

# Performance analysis of port-starboard discrimination for towed multi-line array

Biao Jiang
*Hangzhou Applied Acoustics Research Institute*
*China*

## 1. Introduction

Towed receiving line array has been successfully utilized in military underwater surveillance and seismic exploring. The developments and applications of towed line array sonar can be traced back to 1910s (Lemon, 2004). And the signal processing algorithms for the towed array has been studied extensively in recent a few decades (Nielsen, 1991, Schurman, 1996). Since beampattern of a single-line array is symmetric around the array axis, it cannot tell us whether the target signal is coming from port (left) or from starboard (right), the port-starboard ambiguity is the main shortcoming of a single-line towed array with omni-directional hydrophones. Multi-line array is a simple and convenient way to resolve the problem of port-starboard ambiguity. Considering the system complexity, the twin-line array is the most feasible (Feuillet et al., 1995, Li, 2007) method, triple-line or even larger multi-line array can further improve the detection and localization performance. By now, only twin-line array sonar has been equipped to the surface ships or submarines, there are no reports that triple-line array sonar has been equipped. Triplet array, which uses three closely separated hydrophones acting as a directional sensor, is another solution to the port starboard ambiguity (Groen et al., 2005). The triplet array is easy to be towed and deployed since there is only one tow cable, in spite of its relatively larger diameter. However, because the diameter of triplet array cannot be large enough, it is best applicable to active mode with operational frequency being around 1kHz or higher, not quite satisfactory for low frequency long range passive surveillance. Vector-sensor array is a new method still being studied to achieve port-starboard discrimination (PSD) due to its two-dimensional beampattern in azimuth and elevation (Nehorai & Paldi, 1994, Theriault et. al, 2006). However, the vector-sensor array is very sensitive to the array shape and the installation conditions, so the techniques of vector-sensor have not been so perfect that can be used to fully replace the conventional pressure sensor. Consequently, multi-line array with significantly larger transversal aperture, i.e., the maximum array separation, is promising, especially in littoral environment in which long horizontal single-line array is not appropriate to be used. Multi-line array can also provide vertical aperture to perform range and depth estimation using matched-field processing (MFP). MFP using multi-line array is in research now.

Besides the improved detection capability, port-starboard discrimination is the most important feature of multi-line array. How to evaluate the performance of port-starboard

discrimination is the key to design the multi-line array spatial structure. Left/right suppressed ratio by twin-line array directivity function was commonly used to analyze the left/right ambiguity resolution performance (Li, 2007). Groen used the array gain and port-starboard rejection to analyze the theoretical and experimental performance of three triplet array beamformers: Optimum triplet beamformer, Cardioid beamformer and adaptive triplet beamformer (Groen, 2005). However, these performance analyses are only applicable to the narrowband signal case. For passive sonar, it is desirable to localize the ship radiated wideband noise, so it is important for us to analyze the performance of wideband port starboard discrimination.

In this chapter, we'll discuss the performance of the PSD for the target detected by a towed multi-line array. First, the narrowband port-starboard rejection ratios (PSRR's) are defined and mathematically derived, for both the twin-line array and the triple-line array. Then, the optimum array separation for which the PSRR achieves the maximum is analyzed.

By integrating the narrowband PSRR expression in the processing frequency bandwidth, we obtain the wideband PSRR. Setting the transversal array apertures be equal, the wideband PSRR's of a twin-line array and a triple-line array are compared, and some analytical and simulation results are demonstrated.

Furthermore, two special aspects are studied in this chapter. First, the probability of target the PSD, both narrowband and wideband, for a twin-line array is derived based on the signal detection theory. In a similar way, the probability of PSD for a triple-line array can be obtained. Secondly, the expressions are developed which describe the adaptive port-starboard discrimination for a twin-line array when a correlated interfering signal is present. Conventional beamforming is applied to each line array, followed by a beam-space two-element adaptive beamforming. Then the PSRR is derived in terms of a few parameters, including array separation, signal-to-noise-ratio (SNR), signal-to-interference-ratio (SIR), angular separation and correlation coefficient between the desired signal and the interference. Simulation results are given to demonstrate the results.

## 2. Signal model

Consider a parallel $N$-hydrophone multi-line array with the number of lines $L$, and each of the lines comprises $M$ sensors with inter-element spacing $d$, so that $N=LM$. The transversal array aperture is $D$. Fig. 1 depicts a diagram of a twin-line array. The $j$th sensor on the line $i$ is denoted as $A_{ij}$, and the signal of arrival (DOA) $\theta$ is relative to the front end fire. For convenience, we let $\theta$ be positive in the starboard direction, whereas negative in the port direction.
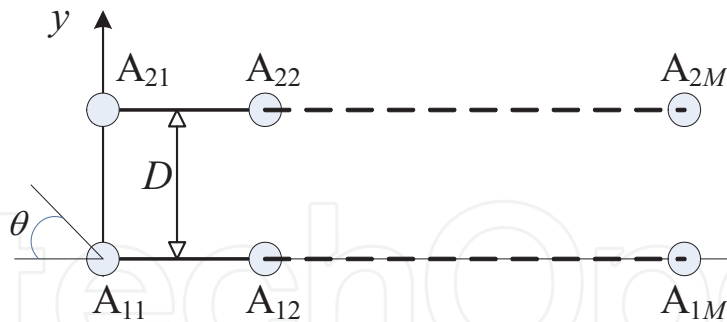
Fig. 1. Diagram of a twin-line array

Assume one narrowband signal with central frequency $f$ impinging on the array, the wavefront propagating speed is $c$, and the array output signal vector can be written as:

$$x(t) = a(\theta)s(t) + n(t) \tag{1}$$

where $s(t)$ denotes the source signal, and $n(t)$ the additive noise vector. $a(\theta)$ is the multi-line array steering vector:

$$a(\theta) = a_T(\theta) \otimes a_L(\theta) \tag{2}$$

where $\otimes$ denotes the Kronecker product. $a_L(\theta)$ is the steering vector of the leftmost line array, and $a_T(\theta)$ is the transversal steering vector, given by:

$$a_L(\theta) = \left[ 1, e^{-j2\pi fd\cos\theta/c}, \cdots, e^{-j2\pi f(M-1)d\cos\theta/c} \right]^T \tag{3}$$

$$a_T(\theta) = [1, e^{j2\pi fD\sin\theta/[c(L-1)]}, \cdots, e^{j2\pi fD\sin\theta/c}]^T \tag{4}$$

## 2.1 Multi-line array directivity

In this section, we'll discuss the directivity functions of two types of multi-line array: twin-line array and triple-line array. When the desired signal direction is $\theta_0$, the normalized multi-line directivity function can be written as (Li, 2007, Nielsen, 1991):

$$
\begin{aligned}
B(f, \theta; \theta_0) &= \frac{1}{LM} \left| a^H(\theta)a(\theta_0) \right| \\
&= \frac{1}{LM} \left| [a_T(\theta) \otimes a_L(\theta)]^H [a_T(\theta_0) \otimes a_L(\theta_0)] \right| \\
&= \frac{1}{LM} \left| a_T^H(\theta)a_T(\theta_0)a_L^H(\theta)a_L(\theta_0) \right|
\end{aligned} \tag{5}
$$

After substituting (3) and (4) to (5) and performing some algebraic manipulation, we get the twin-line and triple-line array directivity functions, as follows

$$B_{\text{twin}}(f, \theta; \theta_0) = \left| \frac{\sin(\pi fMd(\cos\theta - \cos\theta_0)/c)}{M\sin(\pi fd(\cos\theta - \cos\theta_0)/c)} \right| \times \left| \cos[\pi fD(\sin\theta - \sin\theta_0)/c| \tag{6}$$

$$B_{\text{triple}}(f,\theta;\theta_0) = \frac{1}{3} \left| \frac{\sin(\pi f M d(\cos\theta - \cos\theta_0)/c)}{M\sin(\pi f d(\cos\theta - \cos\theta_0)/c)} \right| \times \left| 1 + 2\cos[kD(\sin\theta - \sin\theta_0)/2] \right|$$

(7)

## 2.2 Port-starboard rejection ratio (PSRR)

We use port-starboard rejection ratio to evaluate the performance of port-starboard discrimination. The PSRR is defined as the ratio of the output power in the desired signal direction to that in the mirror direction. Using (6) and (7), we have

$$\text{PSRR}_{\text{twin}} = \frac{\left| B_{\text{twin}}(f,\theta_0;\theta_0) \right|^2}{\left| B_{\text{twin}}(f,-\theta_0;\theta_0) \right|^2} = \frac{1}{\cos^2(2\pi f D \sin\theta_0/c)}$$

(8)

$$\text{PSRR}_{\text{triple}} = \frac{\left| B_{\text{triple}}(f,\theta_0;\theta_0) \right|^2}{\left| B_{\text{triple}}(f,-\theta_0;\theta_0) \right|^2} = \frac{9}{\left| 1 + 2\cos(2\pi f D \sin\theta_0/c) \right|^2}$$

(9)

Consequently, from (8), we can see that, for a desired narrowband signal, when the array spacing is $D = (n \pm 1/4)\lambda/\sin\theta_0, n \in \mathbb{Z}$, where $\lambda$ is the signal wavelength, the twin-line array achieves the maximum PSD performance. Similarly, from (9), the PSRR is optimal for the triple-line array when the transversal aperture satisfies $D = (n \pm 1/3)\lambda/\sin\theta_0, n \in \mathbb{Z}$.

## 2.3 Wideband PSRR

Consider a scenario of one wideband source and noise, the signal is modeled by a white stationary process with power $\sigma_s^2$ with central frequency $f_0$ and bandwidth $B$, and the noise by a spatially white complex process, with power $\sigma_n^2$. Thus, the wideband port-starboard rejection ratios of twin-line and triple-line arrays can be written as

$$\text{PSRR}_{\text{twin}}^{\text{wb}} = \frac{2\int_{f_0-B/2}^{f_0+B/2} \frac{\sigma_s^2}{B} df}{2\int_{f_0-B/2}^{f_0+B/2} \frac{\sigma_s^2}{B}\cos^2(2\pi f D \sin\theta_0/c) df + \sigma_n^2}$$

$$= \frac{2\text{SNR}+1}{\text{SNR}\left[1 + \text{sinc}(\psi B/f_0)\cos(2\psi)\right]+1}$$

(10)

$$\text{PSRR}_{\text{triple}}^{\text{wb}} = \frac{3\int_{f_0-B/2}^{f_0+B/2} \frac{\sigma_s^2}{B} df + \sigma_n^2}{\int_{f_0-B/2}^{f_0+B/2} \frac{\sigma_s^2}{B}[1 + 2\cos(2\pi f D \sin\theta_0/c)]^2/3 df + \sigma_n^2}$$

$$= \frac{3\text{SNR}+1}{\text{SNR}\left\{1+4/3\cos(\psi)\text{sinc}(\psi B/2f_0)+2/3\cos(2\psi)\text{sinc}(\psi B/f_0)\right\}+1} \quad (11)$$

where $\psi = 2\pi Df_0 \sin\theta_0 / c$, $\text{SNR} = \sigma_s^2 / \sigma_n^2$ is the signal-to-noise ratio (SNR). It can be seen from (10), (11) that, the wideband PSRR is mainly determined by the SNR, the transversal aperture, the spectral distribution, and the signal arriving angle. Interestingly, the value of PSRR is independent of the number of sensors of each single-line array.

### 2.4 Simulation results

### 2.4.1 Narrowband beampatterns
In this section, the beampattens of the twin-line array and the triple-line array are presented. The number of elements of each line is $M$=16, Fig. 2 shows the beampatterns of twin-line array and triple-line array by the optimal array separations, for which the PSRR's are maximum for the broadside signals.  Fig. 3 is the transversal cardioid beampatterns, which are the second terms in (6) and (7), of the two multi-line arrays for broadside signals. It's because there is a null in the mirror direction on the cardioid beampattern that the multi-line array can resolve the port-starboard ambiguity.
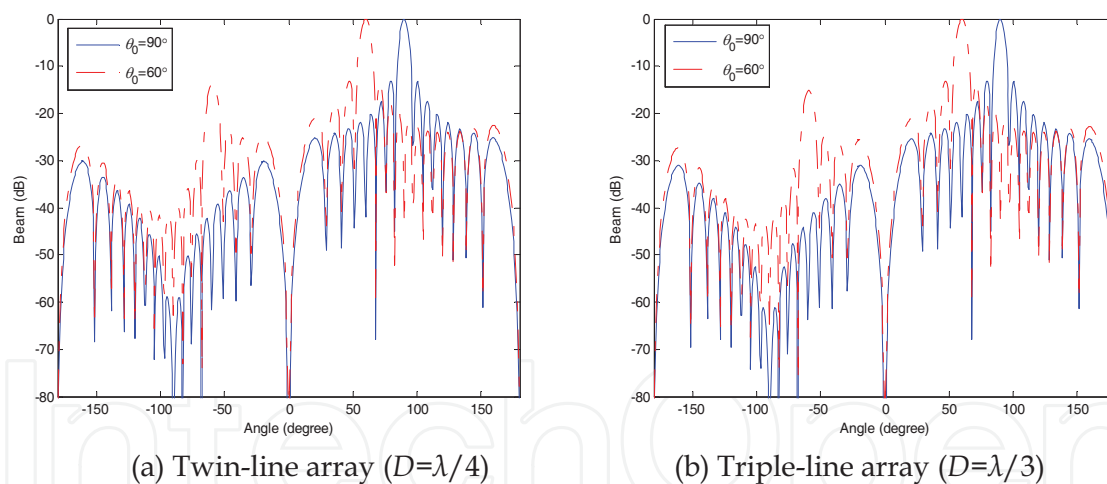In Fig.2, the red line is a dash-dot line as in the word file, in case not to be confused with the blue line.



(a) Twin-line array ($D=\lambda/4$)          (b) Triple-line array ($D=\lambda/3$)
Fig. 2. Beampatterns of the twin-line array and the triple-line array for $M$=16

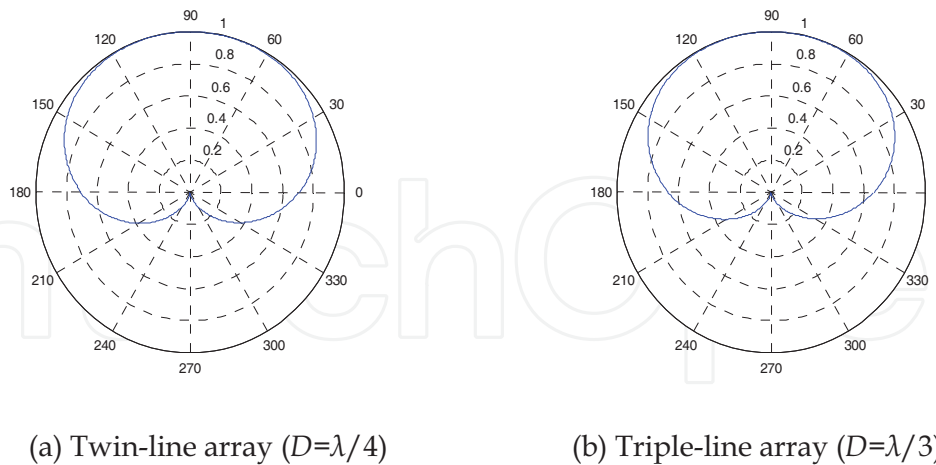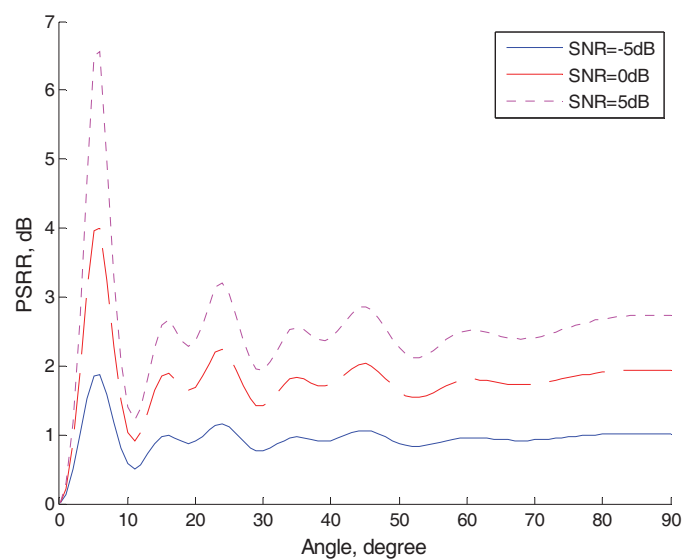(a) Twin-line array (*D=λ/4*)                    (b) Triple-line array (*D=λ/3*)

Fig. 3. Cardioid beampatterns of the twin-line array and the triple-line array for $\theta_0$=90°

### 2.4.2 Wideband PSRR

In this section, the wideband PSRR performance of the twin-line array and the triple-line array is compared. The simulation parameters are $B/f_0$=2/3, $D$=2.5$f_0/c$=2.5$\lambda_0$. Fig. 4 shows the influence of the signal incident angle on the port-starboard discrimination performance. Considering the angular symmetry in (10), (11), only the range of signal arriving angle from 0° to 90° is plotted. From Fig. 4, we observe that, under the condition of equal transversal aperture, the performance of port-starboard discrimination for triple-line array is superior to that of the twin-line array, and the value of PSRR is increasing with the SNR is increasing.

Fig.4 , the three lines are in "solid", "dashed" and "dotted" styles, just as in the word file, when transformed to the pdf file, please assure that they must not be changed to "solid lines" entirely.
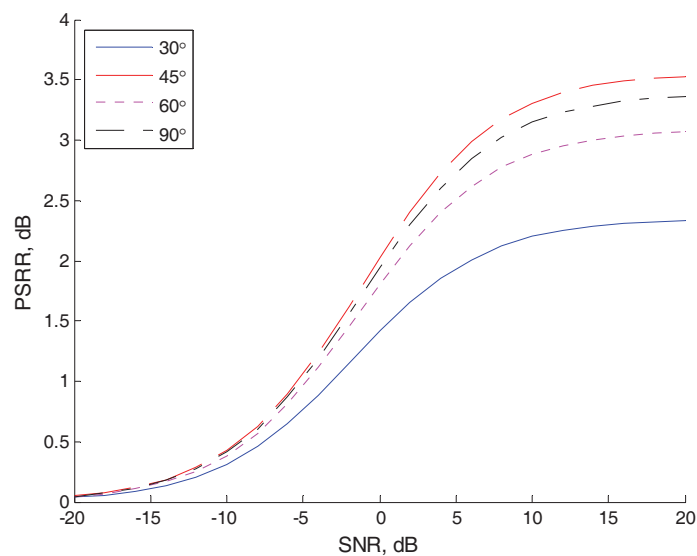


(a) Twin-line array
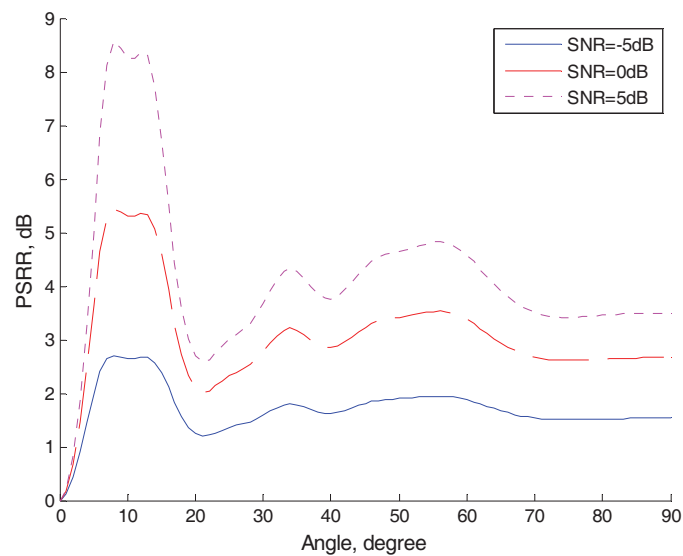
(b) Triple-line array

Fig. 4. Wideband PSRR versus the signal arriving angle

Fig. 5 depicts the wideband PSRR versus the input SNR for different signal arriving angles. It can be seen that, in low SNRs, the PSRR is increasing with the SNR monotonously, and it will level up when the SNR is high enough. Fig. 5 also demonstrates the superiority of the triple-line array in port-starboard discrimination performance than the twin-line array.

The same matter as in Fig.4 is happened in Fig.5, that the four different line styles are all changed to "solid lines" , please check them and revised.



(a) Twin-line array
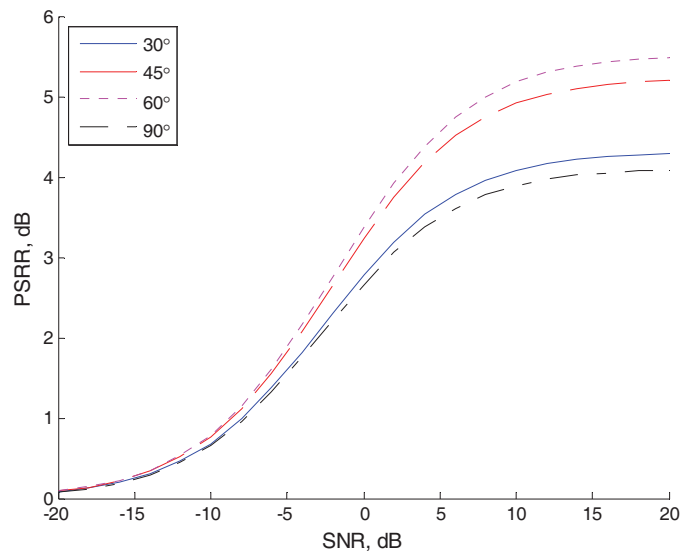
(b) Triple-line array

Fig. 5. Wideband PSRR versus the SNR

## 3. Probability analysis of PSD

Sometimes, it is often be attentioned that how well the PSD is performed over a duration of the observation time. Thus, it is necessary to know the correct probability of source PSD. In this section, the probability of source PSD for underwater towed twin-line array will be derived based on the signal detection theory. The PSD probability of other multi-line can be obtained in the similar way.

### 3.1 Narrowband PSD probability

We use the hypothesis testing theory to decide whether the target signal is coming from port side or starboard side based on the observed data. Using the nomenclature of detection theory, we have to choose between two hypotheses:

$$\text{H}_1: \quad \boldsymbol{x}_1(t) = \boldsymbol{a}_1 s(t) + \boldsymbol{n}(t), \text{ port} \tag{12.1}$$

$$\text{H}_2: \quad \boldsymbol{x}_2(t) = \boldsymbol{a}_2 s(t) + \boldsymbol{n}(t), \text{ starboard} \tag{12.2}$$

where $\boldsymbol{a}_1 = \boldsymbol{a}_T(-\theta) \otimes \boldsymbol{a}_L(\theta)$, $\boldsymbol{a}_2 = \boldsymbol{a}_T(\theta) \otimes \boldsymbol{a}_L(\theta)$ are the array response vector steering to the port side and the starboard side, respectively. The signal and noise are assumed to be mutually uncorrelated zero-mean Gaussian processes. The signal power is $E\{s(t)s^*(t)\} = \sigma_s^2$, and the noise covariance matrix is $E\{\boldsymbol{n}(t)\boldsymbol{n}^H(t)\} = \sigma_n^2 \boldsymbol{I}$.

Let $\boldsymbol{R}_1/\boldsymbol{R}_2$ be the $N \times N$ spatial covariance matrix when $H_1/H_2$ is true. We have

$$\boldsymbol{R}_i = \sigma_s^2 \boldsymbol{a}_i \boldsymbol{a}_i^H + \sigma_n^2 \boldsymbol{I} \quad i = 1, 2 \tag{13}$$

The probability density function (pdf) of $K$ independent data snapshots is given by (Gavish, 1996, Whalen, 1983):

$$\text{H}_1: \quad f(\{\boldsymbol{x}(k)\} \mid \boldsymbol{R}_1) = [\det(\pi \boldsymbol{R}_1)]^{-K} \exp[-K\text{tr}(\boldsymbol{R}_1^{-1}\hat{\boldsymbol{R}})] \tag{14.1}$$

$$\text{H}_2: \quad f(\{x(k)\} \mid R_2) = [\det(\pi R_2)]^{-K} \exp[-K\text{tr}(R_2^{-1}\hat{R})] \tag{14.2}$$

where $\hat{R}$ is the data sample covariance matrix (SCM):

$$\hat{R} = \frac{1}{K}\sum_{k=1}^{K} x(k)x^H(k) \tag{15}$$

To decide between the hypotheses $H_1$ and $H_2$, we form the likelihood ratio:

$$\frac{f(\{x(k)\} \mid R_2)}{f(\{x(k)\} \mid R_1)} \underset{H_1}{\overset{H_2}{\gtrless}} 1 \tag{16}$$

Substituting (14.1) and (14.2) in (16), we obtain the test statistic:

$$\Lambda = \frac{1}{K}\sum_{k=1}^{K} x^H(k)(R_1^{-1} - R_2^{-1})x(k) \underset{H_1}{\overset{H_2}{\gtrless}} \ln\left(\frac{\det(\pi R_2)}{\det(\pi R_1)}\right) = 0 \tag{17}$$

The probability of port-starboard discrimination is defined as the probability of choosing $H_1/H_2$ when $H_1/H_2$ is true, and it can be written as

$$P_{\text{PSD}} = \text{Prob}\{\Lambda < 0 | H_1\} = \text{Prob}\{\Lambda > 0 | H_2\} = \text{erf}(\mu_2 / \delta_2) \tag{18}$$

where $\text{erf}(\cdot)$ is the standard error function defined by

$$\text{erf}(x) = \frac{1}{\sqrt{2\pi}} \int_{-\infty}^{x} e^{-t^2/2} dt \tag{19}$$

and $\mu_2$ and $\delta_2^2$ denote the statistical mean and variance of $\Lambda$ in the case of when $H_2$ is true. When $K$ is large enough, the distribution of $\Lambda$ is approximately normal, and by some algebraic manipulations using (13) and (17), we have

$$\mu_2 = \rho[1 - |\beta|^2] \tag{20}$$

where

$$\rho = \frac{(\|a_2\|^2 \sigma_s^2 / \sigma_n^2)^2}{1 + \|a_2\|^2 \sigma_s^2 / \sigma_n^2} = \frac{(N\sigma_s^2 / \sigma_n^2)^2}{1 + N\sigma_s^2 / \sigma_n^2} \tag{21}$$

$$\beta = a_1^H a_2 / N = (1 + e^{j4\pi D \sin\theta / \lambda})/2 \tag{22}$$

$$\delta_2^2 = \frac{1}{K}\{[\rho(1 - |\beta|^2) + 1]^2 - 1\} \tag{23}$$

Inserting (20)-(23) to (18), we get the probability of PSD:

$$P_{\text{PSD}} = \text{erf}\left[\sqrt{\frac{K}{1 + 2/[\rho(1 - |\beta|^2)]}}\right] \tag{24}$$

From (22) and (24), we can see that for narrowband the signal, the probability of PSD is dependent on the array spacing $D$. For example, when the signal direction is 90°, then the value of $P_{\text{PSD}}$ achieves the maximum when $D = \lambda/4$, and has a minima when $D = \lambda/2$ in which case the array cannot discriminate port from starboard.

### 3.2 Wideband PSD probability

For wideband signal, we assume the signal bandwidth is $[f_l, f_h]$, and there are $N_f$ frequency bins. The probability of PSD in the $k$th frequency bin is denoted by $P_{PSD}(k)$, then two wideband probability of PSD are defined, i.e., the frequency weighting averaged least square (LS) probability estimate and the beam weighting averaged one, which can be written as follows:

$$\hat{P}_{PSD}^{(1)} = \sum_{k=1}^{N_f} f_k^2 P_{PSD}(k) \bigg/ \sum_{k=1}^{N_f} f_k^2 \tag{25}$$

$$\hat{P}_{PSD}^{(2)} = \sum_{k=1}^{N_f} B_L^{\,2}(\theta, f_k) P_{PSD}(k) \bigg/ \sum_{k=1}^{N_f} B_L^{\,2}(\theta, f_k) \tag{26}$$

where $B_L(\theta, f_k)$ is the left array beam power at the steering direction $\theta$, in the $k$th frequency bin. It can be seen from (25) and (26) that, through wideband smoothing, to discriminate port from starboard for wideband signal is less influenced by the array spacing.

### 3.3 Simulation results of PSD probability

Consider an $N$=32 elements twin-line array. The element spacing $d$ is 1m, corresponding to half-wavelength of 750Hz narrowband signal, the number of data snapshots is $K$=100, and 200 independent Monte-Carlo experiments are performed. Fig. 6 shows the probabilities of narrowband port-starboard discrimination versus the signal-to-noise-ratio (SNR). The results are in nice agreement with the theoretical analyses above. If $D=\lambda/4$, the probability of PSD for signal near broadside is greater than from other directions, and the SNR threshold of PSD is lower as well. But when $D=\lambda/2$, the signal from 30° will attain the best port-starboard discrimination performance, and the broadside signal has the port-starboard ambiguity, as can be seen from (24).
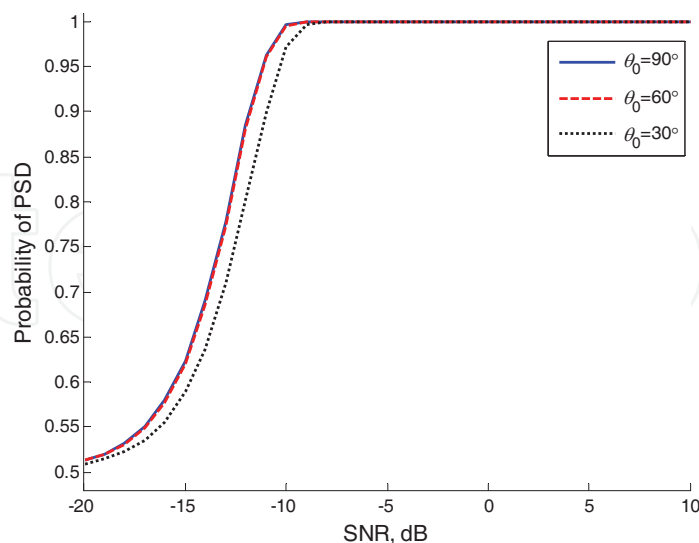


(a) $D$=0.5m (a quarter of the signal wavelength)
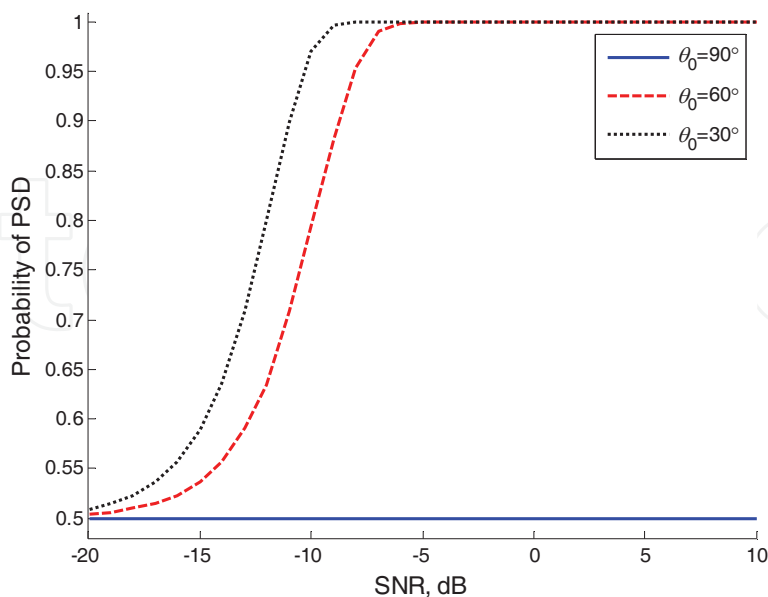
(b) *D*=1m (half of the signal wavelength)
Fig. 6. Probabilities of narrowband port-starboard discrimination versus the SNR

Fig. 7 depicts the probability of PSD for wideband signal. The source signal is assumed to be band-limited Gaussian process with flat spectra from 400Hz to 750Hz. The signal frequency band is divided into $N_f$=31 subbands. The twin-array spacing is set to be 6m. Fig. 7 demonstrates the robustness of wideband port-starboard discrimination to the array spacing.
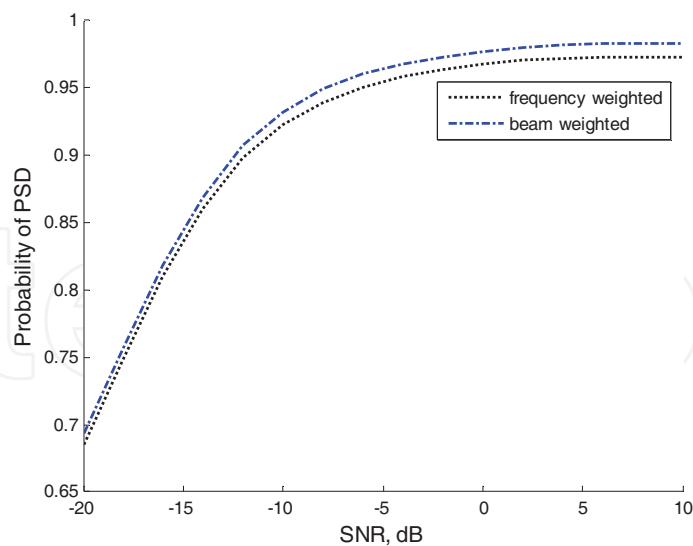


Fig. 7. Probabilities of wideband port-starboard discrimination versus the SNR

## 4. General PSRR analysis for twin-line array

In section 2, the narrowband PSRR is analyzed in noise-free scenarios, which exhibits an optimal PSD performance. The SNR is considered in wideband PSRR performance analysis, and it was shown that the PSRR performance is improved with the SNR.

In fact, the PSRR is determined by a lot of parameters. Besides the array separation, other parameters including the SNR, the interference-to-noise-ratio (INR), the signal-to-interference-ratio (SIR), the angular separation and correlation between the desired signal and the interference, the array size and the finite sample size.

In this section, we will present a complete analysis of the PSRR as a function of a few important parameters which may affect the PSD performance. With no loss of generality, the twin-line array is considered here.

### 4.1 General signal model in the presence of interferences

Consider a totally $N$-hydrophone ($N=2M$) twin-line array towed in the horizontal $x$-$y$ plane in the direction of decreasing $x$, and $D$ denotes the array separation, and other parameters defined as in section 2. The array received $N \times 1$ signal vector $x(t)$ can be written as

$$\boldsymbol{x}(t) = \boldsymbol{a}(\theta_1)s_1(t) + \boldsymbol{v}(t) \tag{27}$$

where $v(t)$ denotes the interference-plus-noise vector, and it can be written as (Wax and Anu, 1996)

$$\boldsymbol{v}(t) = \sum_{k=2}^{q} \boldsymbol{a}(\theta_k)s_k(t) + \boldsymbol{n}(t) \tag{28}$$

where $s_k(t)$ denotes the signal of the $k$th source, and $n(t)$ is the additive Gaussian noise vector, and $a$ is as (2).

The output of the conventional plane-wave beamforming is given by

$$y(t) = \boldsymbol{w}^H \boldsymbol{x}(t) \tag{29}$$

where $w$ is the weight vector, for conventional delay-and-sum beamforming, $w$ is the same as the steering vector toward the desired signal.

From (27), we can express the sample covariance matrix (SCM) as (Wax and Anu, 1996, Raghunath & Reddy, 1992):

$$\hat{\boldsymbol{R}} = \frac{1}{K}\sum_{t=1}^{K} \boldsymbol{x}(t)\boldsymbol{x}^H(t) = \hat{\sigma}_{s_1}^2 \boldsymbol{a}_1 \boldsymbol{a}_1^H + \boldsymbol{a}_1 \hat{\boldsymbol{r}}^H + \hat{\boldsymbol{r}} \boldsymbol{a}_1^H + \hat{\boldsymbol{Q}} \tag{30}$$

where $K$ is the number of samples, $a_1$ is the abbreviation for $a(\theta_1)$, and $\hat{\sigma}_{s_1}^2$ denotes the sample-mean of the desired signal power:

$$\hat{\sigma}_{s_1}^2 = \frac{1}{K}\sum_{t=1}^{K} |s_1(t)|^2 \tag{31}$$

where $\hat{\boldsymbol{r}}$ denotes the sample-mean of the correlation between the desired signal and the interference-plus-noise:

$$\hat{\boldsymbol{r}} = \frac{1}{K}\sum_{t=1}^{K} s_1^*(t)\boldsymbol{v}(t) \tag{32}$$

and $\hat{Q}$ is the sample covariance matrix of the interference-plus-noise

$$\hat{Q} = \frac{1}{K} \sum_{t=1}^{K} \boldsymbol{v}(t) \boldsymbol{v}^H(t) \tag{33}$$

Now we redefine the PSRR as the ratio between the practical output power toward the desired signal arriving direction and that in the back-beam direction, as follows

$$\widehat{\mathrm{PSRR}} = \frac{\boldsymbol{w}_+^H \hat{\boldsymbol{R}} \boldsymbol{w}_+}{\boldsymbol{w}_-^H \hat{\boldsymbol{R}} \boldsymbol{w}_-} \tag{34}$$

where $w_+$ and $w_-$ denote the weight vector steered to the desired signal direction and to the mirror signal direction, respectively. For conventional beamforming, $w_+ = a_1$, and $w_- = a_{1-}$, here $a_{1-}$ stands for $a(-\theta_1)$, then (33) can be rewritten as

$$\widehat{\mathrm{PSRR}} = \frac{\boldsymbol{a}_1^H \hat{\boldsymbol{R}} \boldsymbol{a}_1}{\boldsymbol{a}_{1-}^H \hat{\boldsymbol{R}} \boldsymbol{a}_{1-}} = \frac{\boldsymbol{a}_1^H [\hat{\sigma}_{s_1}^2 \boldsymbol{a}_1 \boldsymbol{a}_1^H + \boldsymbol{a}_1 \hat{\boldsymbol{r}}^H + \hat{\boldsymbol{r}} \boldsymbol{a}_1^H + \hat{\boldsymbol{Q}}] \boldsymbol{a}_1}{\boldsymbol{a}_{1-}^H [\hat{\sigma}_{s_1}^2 \boldsymbol{a}_1 \boldsymbol{a}_1^H + \boldsymbol{a}_1 \hat{\boldsymbol{r}}^H + \hat{\boldsymbol{r}} \boldsymbol{a}_1^H + \hat{\boldsymbol{Q}}] \boldsymbol{a}_{1-}}$$

$$= \frac{\hat{\sigma}_{s_1}^2 N^2 + 2N \,\mathrm{Re}(\boldsymbol{a}_1^H \hat{\boldsymbol{r}}) + \boldsymbol{a}_1^H \hat{\boldsymbol{Q}} \boldsymbol{a}_1}{\hat{\sigma}_{s_1}^2 |\boldsymbol{a}_{1-}^H \boldsymbol{a}_1|^2 + 2\,\mathrm{Re}(\boldsymbol{a}_{1-}^H \hat{\boldsymbol{r}} \boldsymbol{a}_1^H \boldsymbol{a}_{1-}) + \boldsymbol{a}_{1-}^H \hat{\boldsymbol{Q}} \boldsymbol{a}_{1-}} \tag{35}$$

where $\mathrm{Re}(\cdot)$ means the real part, and

$$|\boldsymbol{a}_{1-}^H \boldsymbol{a}_1| = N \cos(2\pi f D \sin\theta_1 / c) \tag{36}$$

Substituting (28) into (32), we have

$$\hat{\boldsymbol{r}} = \sum_{k=2}^{q} \boldsymbol{a}(\theta_k) \left( \frac{1}{K} \sum_{t=1}^{K} s_1^*(t) s_k(t) \right) + \frac{1}{K} \sum_{t=1}^{K} s_1^*(t) \boldsymbol{n}(t)$$

$$= \sum_{k=2}^{q} \boldsymbol{a}(\theta_k) \hat{\sigma}_{s_1} \hat{\sigma}_{s_k} \hat{\rho}_{1k} + \hat{\sigma}_{s_1} \hat{\boldsymbol{\sigma}}_n \odot \hat{\boldsymbol{\rho}}_{1n} \tag{37}$$

where $\hat{\rho}_{1k}$ is the sample-mean of the correlation coefficient between $s_1(t)$ and $s_k(t)$, $\hat{\boldsymbol{\sigma}}_n$ is the noise standard deviation vector, and $\hat{\boldsymbol{\rho}}_{1n}$ is the sample-mean of the correlation coefficient vector between $s_1(t)$ and $\boldsymbol{n}(t)$, $\odot$ denotes the element-wise vector or matrix product. When the desired signal and the noise is uncorrelated, then the second term in (37) can be omitted. From (35) and (37), we can see that the performance of port-starboard discrimination is determined by a few parameters, such as the power of the desired signal, the interference and noise, the correlation between the desired signal and the interference, the array separation, and so on.


## 4.2 Theoretical PSRR in some special cases
In section 4.1, we obtain the sample-based expression for PSRR, see (35). Now, replacing the sample covariance matrix $\hat{\boldsymbol{R}}$ with the exact covariance matrix $\boldsymbol{R}$, we obtain the theoretical PSRR expression for large sample condition. The expectation of (35) can be written as

$$\text{PSRR} = \frac{\boldsymbol{w}_+^H \boldsymbol{R} \boldsymbol{w}_+}{\boldsymbol{w}_-^H \boldsymbol{R} \boldsymbol{w}_-} = \frac{\sigma_{s_1}^2 N^2 + 2N \operatorname{Re}(\boldsymbol{a}_1^H \boldsymbol{r}) + \boldsymbol{a}_1^H \boldsymbol{Q} \boldsymbol{a}_1}{\sigma_{s_1}^2 |\boldsymbol{a}_{1-}^H \boldsymbol{a}_1|^2 + 2 \operatorname{Re}(\boldsymbol{a}_{1-}^H \boldsymbol{r} \boldsymbol{a}_1^H \boldsymbol{a}_{1-}) + \boldsymbol{a}_{1-}^H \boldsymbol{Q} \boldsymbol{a}_{1-}} \tag{38}$$

### 4.2.1 Desired signal only

In the case that only the desired signal is present, we have

$$\boldsymbol{v}(t) = \boldsymbol{n}(t) \tag{39}$$

Assume $\boldsymbol{n}(t)$ is independent of $s_1(t)$, and has zero mean and covariance matrix $\sigma_n^2 \boldsymbol{I}$, it gives

$$\boldsymbol{r} = E\{s_1^*(t)\boldsymbol{v}(t)\} = E\{s_1^*(t)\boldsymbol{n}(t)\} = \boldsymbol{0} \tag{40}$$

where $\boldsymbol{0}$ is a all-zero vector, and

$$\boldsymbol{Q} = E\{\boldsymbol{n}(t)\boldsymbol{n}^H(t)\} = \sigma_n^2 \boldsymbol{I} \tag{41}$$

Substituting (39)–(40) into (38), and after some algebraic manipulation, we readily get

$$\text{PSRR} = \frac{N\sigma_{s_1}^2 + \sigma_n^2}{N\sigma_{s_1}^2 \cos^2(2\pi f D \sin\theta_1 / c) + \sigma_n^2} \tag{42}$$

Denoting by SNR as the signal-to-noise ratio of the desired signal at a single omnidirectional sensor

$$\text{SNR} = \frac{\sigma_{s_1}^2}{\sigma_n^2} \tag{43}$$

we can rewrite (42) as

$$\text{PSRR} = \frac{N\text{SNR} + 1}{N\text{SNR}\cos^2(2\pi f D \sin\theta_1 / c) + 1}. \tag{44}$$

Thus, for the SNR is fixed, we have

$$1 \le \text{PSRR} \le N\text{SNR} + 1 \tag{45}$$

and for fixed $D$, $f$ and $\theta_1$, when

$$\text{SNR} \gg 1 / [N\cos^2(2\pi f D \sin\theta_1 / c)],$$

we have

$$\text{PSRR} \simeq \frac{1}{\cos^2(2\pi f D \sin\theta_1 / c)} \tag{46}$$

that is, (44) is reduced to (8), while for

$$\text{SNR} \ll 1 / [N\cos^2(2\pi f D \sin\theta_1 / c)],$$

we have

$$\text{PSRR} \simeq N\text{SNR} + 1 \tag{47}$$

From (46) and (47), we can conclude that, the PSRR is linearly increasing with SNR up to (46) where it levels up and fixed.

### 4.2.2 Desired signal and a single interference
In the case of a single interference, we have

$$v(t) = a_2 s_2(t) + n(t) \tag{48}$$

and also, $n(t)$ is independent of $s_2(t)$ and has zero mean and covariance matrix $\sigma_n^2 I$, then

$$r = E\{s_1^*(t)v(t)\} = a_2 E\{s_1^*(t)s_2(t)\} = a_2 \sigma_{s_1} \sigma_{s_2} \rho_{12} \tag{49}$$

where $\rho_{12}$ is the correlation coefficient between $s_1(t)$ and $s_2(t)$

$$\rho_{12} = \frac{E\{s_1^*(t)s_2(t)\}}{\sigma_{s_1} \sigma_{s_2}} \tag{50}$$

And

$$Q = \sigma_{s_2}^2 a_2 a_2^H + \sigma_n^2 I . \tag{51}$$

Using (2) and (49), we can get

$$\text{Re}(a_1^H r) = \sigma_{s_1} \sigma_{s_2} \text{Re}(a_1^H a_2 \rho_{12}) = N \sigma_{s_1} \sigma_{s_2} \text{Re}(\alpha \rho_{12}) \tag{52}$$

$$a_1^H Q a_1 = \sigma_{s_2}^2 N^2 |\alpha|^2 + N \sigma_n^2 \tag{53}$$

$$a_{1-}^H Q a_{1-} = \sigma_{s_2}^2 |a_{1-}^H a_2|^2 + N \sigma_n^2 \tag{54}$$

where

$$\alpha = a_1^H a_2 / |a_1||a_2| = a_1^H a_2 / N \tag{55}$$

is a complex scalar characterizes the *spatial correlation coefficient* between the steering vectors of the desired signal and the interference. And using (2)–(4), we readily have

$$
\begin{aligned}
a_{1-}^H a_2 / N &= a_T^H(-\theta_1)a_T(\theta_2)a_L^H(-\theta_1)a_L(\theta_2) / N \\
&= a_T^H(-\theta_1)a_T(\theta_2)a_L^H(\theta_1)a_L(\theta_2) / N \\
&= e^{jk(M-1)d(\cos\theta_1 - \cos\theta_2)/2} \frac{\sin(kMd(\cos\theta_1 - \cos\theta_2)/2)}{M \sin(kd(\cos\theta_1 - \cos\theta_2)/2)}
\end{aligned}
$$

$$\times e^{jkD(\sin\theta_1 + \sin\theta_2)/2} \cos[kD(\sin\theta_1 + \sin\theta_2)/2] = B(f, -\theta_1; \theta_2) \tag{56}$$

So, we get

$$|a_{1-}^H a_1|^2 / N^2 = \cos^2(kD \sin\theta_1) \tag{57}$$

$$\frac{\text{Re}(a_{1-}^H r a_1^H a_{1-})}{N^2} = \sigma_{s_1} \sigma_{s_2} \beta \tag{58}$$

and $\beta$ is derived as

$$\beta = \cos(kD \sin\theta_1) \cos[kD(\sin\theta_1 + \sin\theta_2)/2] \frac{\sin(kMd(\cos\theta_1 - \cos\theta_2)/2)}{M \sin(kd(\cos\theta_1 - \cos\theta_2)/2)}$$

$$\times \text{Re}\left\{\rho_{12}e^{jk[(M-1)d(\cos\theta_1-\cos\theta_2)-D(\sin\theta_1-\sin\theta_2)]/2}\right\} \tag{59}$$

Substituting the results (52)–(59) into (38), and let both the nominator and denominator be divided by $N^2$, we get

$$\text{PSRR} = \frac{P_+}{P_-} \tag{60}$$

where

$$P_+ = \sigma_{s_1}^2 + 2\sigma_{s_1}\sigma_{s_2}\text{Re}(\alpha\rho_{12}) + \sigma_{s_2}^2 |\alpha|^2 + \sigma_n^2 / N \tag{61}$$

$$P_- = \sigma_{s_1}^2 \cos^2(kD\sin\theta_1) + 2\sigma_{s_1}\sigma_{s_2}\beta + \sigma_{s_2}^2 |B(f,-\theta_1;\theta_2)|^2 + \sigma_n^2 / N \tag{62}$$

Let $\text{INR} = \sigma_{s_1}^2 / \sigma_n^2$ denote the interference-to-noise ratio, and then dividing (61) and (62) by $\sigma_n^2$, we get

$$P_+ = \text{SNR} + 2\sqrt{\text{SNR}\cdot\text{INR}}\,\text{Re}(\alpha\rho_{12}) + \text{INR}\,|\alpha|^2 + 1/N \tag{63}$$

$$P_- = \text{SNR}\cos^2(kD\sin\theta_1) + 2\sqrt{\text{SNR}\cdot\text{INR}}\,\beta$$
$$+ \text{INR}\,|B(f,-\theta_1;\theta_2)|^2 + 1/N \tag{64}$$

That is, the PSRR is affected by a few parameters in practice, such as the SNR, the INR, or signal-to-interference ratio (SIR, SIR=SNR/INR), the correlation coefficient between the desired signal and the interference, the spatial correlation coefficient related to the angular separation between the desired signal and the interference, array separation and the array size, *etc*.

From (63)–(64), when the INR is much smaller than the SNR, or when the spatial correlation coefficient $\alpha$ approaches zero, then (60) will reduce to (44).

### 4.3 Simulation results

In our simulations, we consider an $N$=32 twin-line array with half-wavelength inter-element spacing, and the array separation is a quarter of wavelength. The experimental results were computed using (35) by 100 Monte-Carlo runs, and the analytical results were computed by (60), (63)–(64), the number of samples is 100.

In the first experiment, we consider that there is a correlated interference near the front endfire with direction 20°, and the desired signal is in the broadside, i.e. $\theta_1$=90°.

Fig. 8 shows the analytical PSRR and simulated experimental PSRR versus the input SNR, for SIR=20dB and SIR=–20dB, respectively. For high SIR, the analytical curve coincides with the practical result precisely, and we can obtain the satisfactory port-starboard discrimination performance. However, when there are strong interferences, the PSRR can not increase with SNR, and it will level up when the SNR is large enough.

In the second experiment, we consider the effect of the correlation between the desired signal and the interference, to the value of the PSRR. Fig. 9 depicts the resulting PSRR versus the SNR. For low SIR, the PSRR will decrease when the interference is correlated with the desired signal, while the correlation has little effect to the PSRR for high SIR.
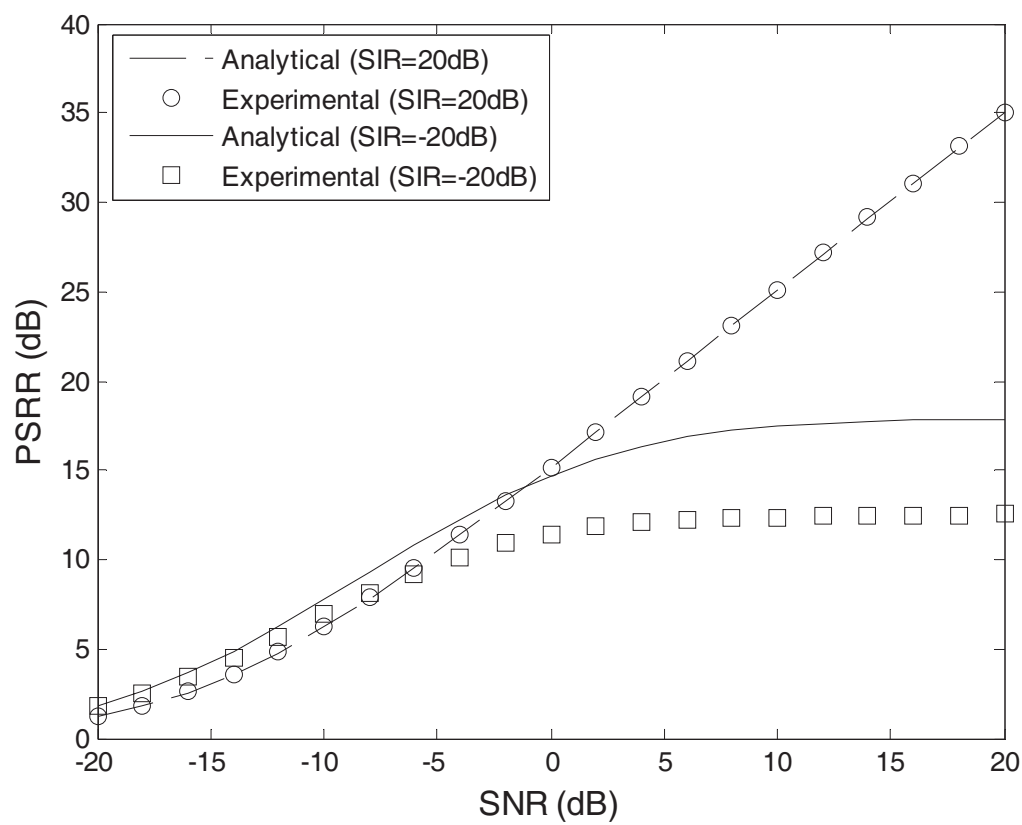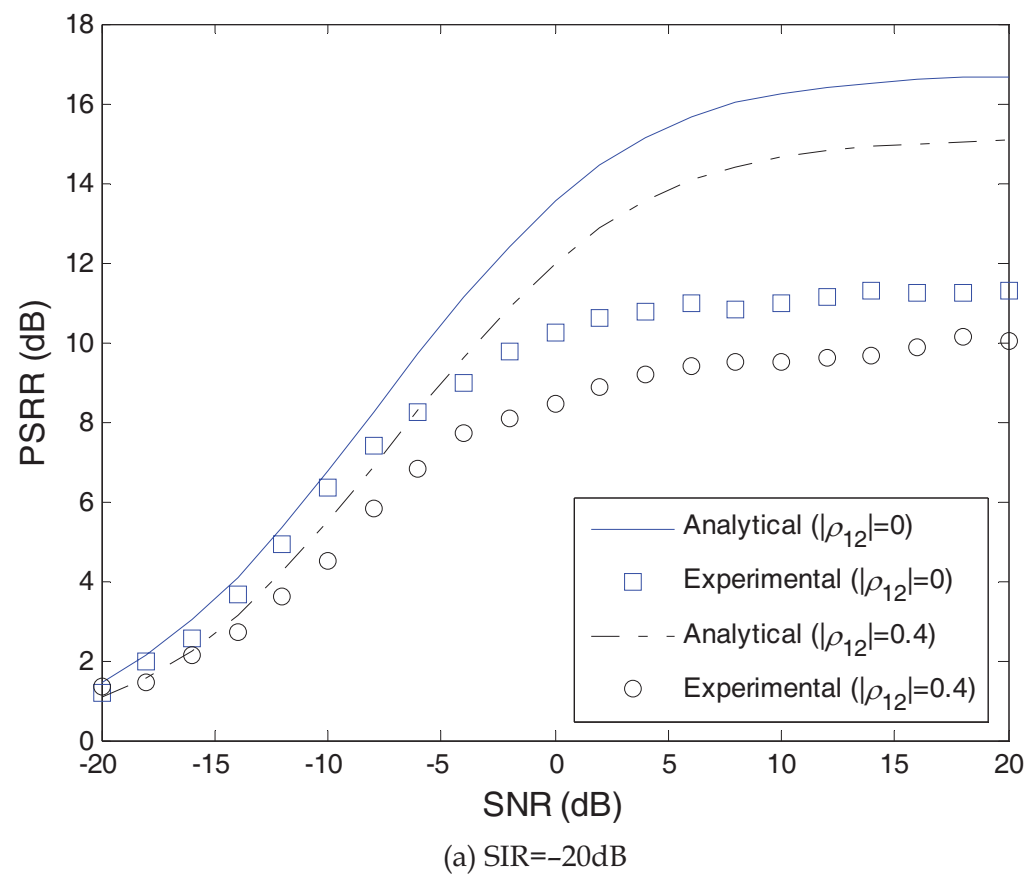
Fig. 8. The PSRR of the desired signal versus the SNR ($D=\lambda/4$, $\theta_1=90°$, $\theta_2=20°$, $|\rho 12|=0.4$)
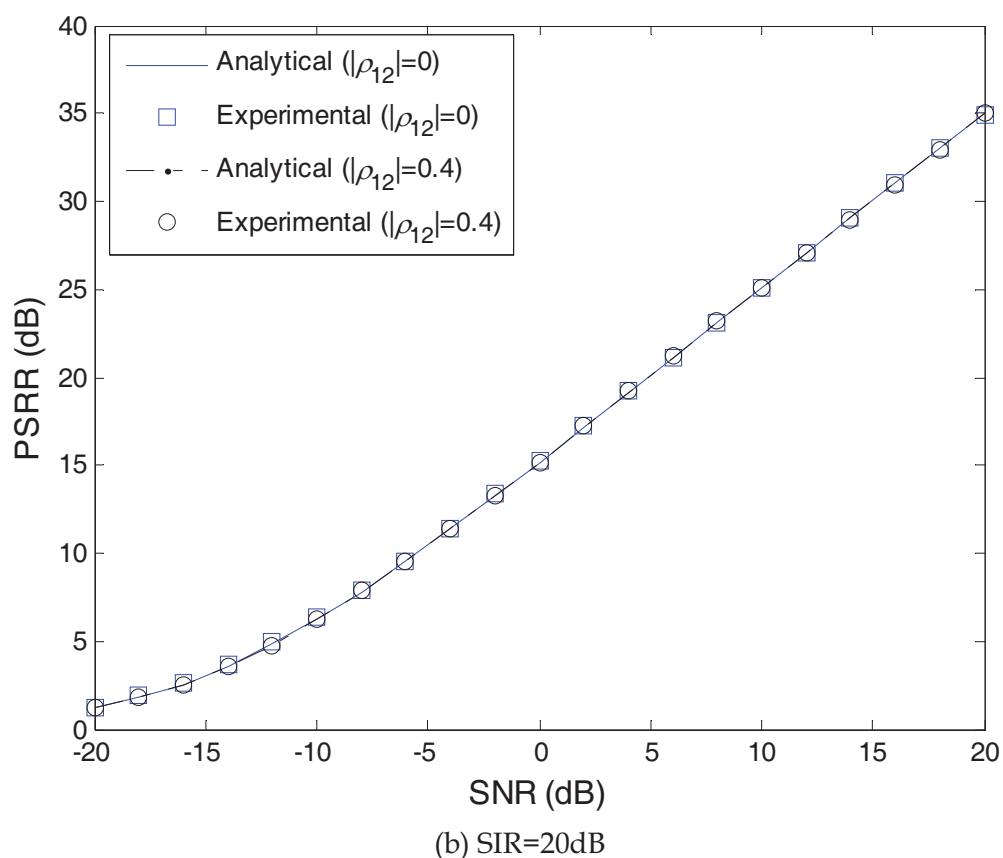
(a) SIR=–20dB

(b) SIR=20dB

Fig. 9.  The PSRR of the desired signal versus the SNR ($D=\lambda/4$, $\theta_1=90°$, $\theta_2=20°$)

Numerical results demonstrate that the PSRR performance was mainly affected by the array separation, the signal-to-interference ratio, the correlation between the desired signal and the interference, and the SNR.

## 5. Conclusion

In this chapter, we have discussed the issue of the target signal port-starboard discrimination (PSD) for underwater towed multi-line array. The port-starboard rejection ratios (PSRR's) are defined to evaluate the PSD performance, for both narrowband and wideband signals. The optimum array separations with perfect PSD performance are proposed. And the closed forms of the wideband PSRR's are derived in this chapter, it was pointed out that the wideband PSRR of the triple-line array is greater than that of the twin-line array under the condition of equal transversal aperture.

The narrowband and wideband PSD probability for the twin-line array are derived based on the signal detection theory. The analytical and simulation results show that the wideband PSD probability is robust to the array separation. Furthermore, the general PSRR expressions are developed in the presence of a correlated interfering signal. The results show that a lot of parameters together determine the PSD performance, such as the array separation, the SNR, the SIR, the angular separation and the correlation coefficient between the desired signal and the interference.

In a word, the theoretical and numerical analyses of the multi-line array PSD performance are in detail. However, more lake trial or sea trial data are needed to validate the practical PSD performance, and to compare with the theoretical performance. We have been researching and developing the multi-line array, and the experimental results will be provided later.

## 6. References

Cox, H. et al (2003). Hybrid adaptive beamforming for multi-line arrays. *Proc. 37th Asilomar Conf. on Signals, Systems and Computers*. pp. 1858-1862, Vol. 2, Nov

Doisy, Y. (1995). Port-starboard discrimination performances on active towed array systems, *Proc. Underwater Defense Technology (UDT)*, pp. 125-129, Cannes, France

Feuillet, J. P.; Allensworth, W. S.; & Newhall, B. K. (1995). Nonambiguous beamforming for a high resolution twin-line array. *J. Acoust. Soc. Amer.*, Vol. 97, No. 5, p. 3292

Gavish, M. & Weiss, A. J. (1996). Array Geometry for ambiguity resolution in direction finding. *IEEE Trans. Antennas Propag.*, Vol. 44, No. 6, pp. 889–895

Groen, J.; Beerens, S. P.; & Doisy, Y. (2005). Adaptive port-starboard beamforming of triplet sonar arrays. *IEEE J. of Oceanic Eng.*, Vol. 30, No. 2, pp. 348–359

Lemon, S. G. (2004). Towed-array History, 1917–2003. *IEEE J. of Oceanic Eng.*, Vol. 29, No. 2, pp. 365–373

Li, Q. H. (2007). Preliminary analysis of left-right ambiguity resolution performance for twin-line array. *Chinese Journal of Acoustics*, Vol. 26, No. 1, pp. 1–6

Nehorai, A. & Paldi E. (1994). Acoustic vector-sensor array processing. *IEEE Trans. Signal Process.*, Vol. 42, No. 9, pp. 2481–2491

Nielsen, R. O. (1991). *Sonar Signal Processing*. Norwood, MA: Artech House, Boston

Raghunath, K. J. & Reddy, V. U. (1992). Finite data performance analysis of MVDR beamformer with and without spatial smoothing. *IEEE Trans. Signal Process.*, Vol. 40, No. 11, pp. 2726–2736

Schurman, I. W. (1996). Reverberation rejection with a dual-line towed array. *IEEE J. of Oceanic Eng.*, Vol. 21, No. 2, pp. 193–204

Theriault, J. A. et al. (2006). Performance comparison of arrays of directional versus omnidirectional sensors using base '04 data. *Proc. 8th European Conference on Underwater Acoustics (8th ECUA)*, 12-15, June, Carvoeiro, Portugal

Wax, M. & Anu, Y. (1996). Performance analysis of the minimum variance beamformer. *IEEE Trans. Signal Process.*, Vol. 44, pp. 928–937, Apr. 1996

Whalen, A. D. (1983). *Detection of signals in noise*. Academic Press, New York
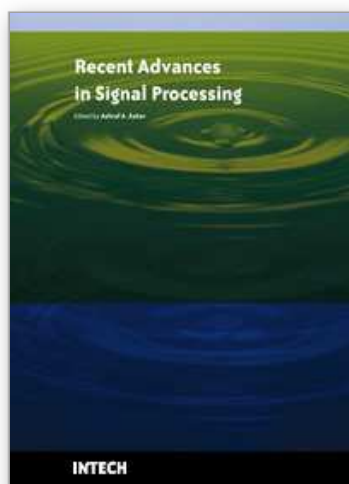
**Recent Advances in Signal Processing**

Edited by Ashraf A Zaher

The signal processing task is a very critical issue in the majority of new technological inventions and challenges in a variety of applications in both science and engineering fields. Classical signal processing techniques have largely worked with mathematical models that are linear, local, stationary, and Gaussian. They have always favored closed-form tractability over real-world accuracy. These constraints were imposed by the lack of powerful computing tools. During the last few decades, signal processing theories, developments, and applications have matured rapidly and now include tools from many areas of mathematics, computer science, physics, and engineering. This book is targeted primarily toward both students and researchers who want to be exposed to a wide variety of signal processing techniques and algorithms. It includes 27 chapters that can be categorized into five different areas depending on the application at hand. These five categories are ordered to address image processing, speech processing, communication systems, time-series analysis, and educational packages respectively. The book has the advantage of providing a collection of applications that are completely independent and self-contained; thus, the interested reader can choose any chapter and skip to another without losing continuity.

**How to reference**

In order to correctly reference this scholarly work, feel free to copy and paste the following:

Biao Jiang (2009). Performance Analysis of Port-Starboard Discrimination for Towed Multi-Line Array, Recent Advances in Signal Processing, Ashraf A Zaher (Ed.), ISBN: 978-953-307-002-5, InTech, Available from: http://www.intechopen.com/books/recent-advances-in-signal-processing/performance-analysis-of-port-starboard-discrimination-for-towed-multi-line-array

# INTECH
open science | open minds